

Optical spectroscopy of galaxies in the direction of the Virgo cluster. ^{*}

Giuseppe Gavazzi¹, Christian Bonfanti¹, Paola Pedotti¹, Alessandro Boselli², and Luis Carrasco^{3,4}

¹ Università degli Studi di Milano - Bicocca, P.zza dell'Ateneo Nuovo 1, 20126 Milano, Italy.

² Laboratoire d'Astronomie Spatiale, Traverse du Siphon, F-13376 Marseille Cedex 12, France.

³ Instituto Nacional de Astrofísica, Óptica y Electrónica, Apartado Postal 51. C.P. 72000 Puebla, Pue., México

⁴ Observatorio Astronómico Nacional/UNAM, Ensenada B.C., México

October 27, 2018

Abstract. Optical spectroscopy of 76 galaxies, 48 of which are projected in the direction of the Virgo cluster and 28 onto the Coma–A1367 supercluster, is reported. Adding these new measurements to those found in the literature, the redshift completeness in the Virgo region becomes 92 % at $B_T \leq 16.0$ and 68 % at $B_T \leq 18.0$. The one of CGCG galaxies in the direction of the Coma–A1367 supercluster becomes 98 %. The Virgo cluster membership estimates obtained on morphological grounds by Binggeli et al. (1985) are confirmed in all cases. However, several “possible members” classified as BCD (if in the cluster) are found instead to be giant emission-line galaxies in the background of the Virgo cluster

Key words: galaxies: redshift; galaxies: large-scale structure; galaxies: clusters: individual: Virgo

1. Introduction

The Virgo cluster, the nearest rich cluster of galaxies in the northern hemisphere, was surveyed with unprecedented resolution and completeness in the extensive photographic survey carried out with the DuPont telescope at Las Campanas. Based on this material Binggeli et al. (1985) compiled the Virgo Cluster Catalogue (VCC), which lists 2096 galaxies brighter than $B_T \leq 20.0$ (1323 of which constitute a complete subsample to $B_T \leq 18.0$). This work has served to many important developments, in particular for mapping for the first time the luminosity function of

a cluster down to $M_p = -13.1$ (assuming a distance modulus of Virgo $\mu = -31.1$, corresponding to the distance of 17 Mpc; see Gavazzi et al. 1999a) and for comparing the various luminosity functions across the entire Hubble sequence (Sandage, Binggeli, & Tammann, 1985). In absence of a complete redshift information (by the time of its publication only about 30% VCC galaxies had an actual redshift measurement), the cluster membership was assigned to the individual objects on a purely morphological (surface brightness) basis. Since then the number of available redshifts either from optical (e.g. Binggeli et al. 1993, Grogin, Geller, & Huchra 1998; hereafter GGH98) or from radio spectroscopy (e.g. Haynes & Giovanelli 1986, Hoffman et al. 1987, Hoffman et al. 1989, Hoffman et al. 1995, Magri 1994) has increased considerably. Nonetheless the present redshift completeness in this region is still only 65% at $B_T \leq 18.0$.

A better redshift completeness exists in the Coma–A1367 supercluster region $11^h30^m < \alpha < 13^h30^m; 18^\circ < \delta < 32^\circ$, limited however to the shallower magnitude limit of 15.7 of the CGCG catalogue (Zwicky et al. 1961–68). Gavazzi et al. (1999b) counted 1068 redshift measurements out of 1127 CGCG galaxies listed in this region. With the aim of contributing with new redshift measurements in these regions we undertook the spectroscopic survey presented in this paper, which was carried out during marginally photometric nights. The observations and data reduction are presented in section 2. The new redshifts are given and discussed in section 3.

2. Observations and data reduction

Galaxies in the present study were primarily selected among the objects brighter than $B_T \leq 17.0$ in the VCC Catalogue of Virgo Cluster galaxies by Binggeli et al. (1985). CGCG (Zwicky et al. 1961–68) galaxies in the region $11^h30^m < \alpha < 13^h30^m; 18^\circ < \delta < 32^\circ$, containing the Coma–A1367 supercluster, were also selected as filler

Send offprint requests to: Gavazzi@uni.mi.astro.it

^{*} Based on observations obtained with the Loiano telescope belonging to the University of Bologna (Italy), with the OHP, operated by the French CNRS and with the G. Haro telescope of the INAOE (Mexico)

Table 1. The spectrograph characteristics

Telescope	<i>run</i>	<i>Spectrograph</i>	<i>dispersion</i> Å/mm	<i>coverage</i> Å	<i>CCDtype</i>	<i>pix</i> μm
Loiano	<i>Jan – Feb</i> 1999	<i>BFOSC</i>	198	4060 – 7900	1024 × 1024 <i>TH</i>	19
Loiano	<i>Jan – Feb</i> 2000	<i>BFOSC</i>	198	3600 – 8900	1340 × 1300 <i>EEV</i>	20
Cananea	<i>Apr</i> 2000	<i>LFOSC</i>	228	4000 – 7100	576 × 384 <i>TH</i>	23
OHP	<i>Mar</i> 1999	<i>CARELEC</i>	133	3200 – 7100	2048 × 1024 <i>EEV</i>	13.5

objects. Long-slit, low dispersion spectra of 76 galaxies were obtained in several observing runs since 1999 using the imaging spectrographs BFOSC and LFOSC attached to the Cassini 1.5 m telescope at Loiano (Italy), to the 2.1 m telescope of the Guillermo Haro Observatory at Cananea (Mexico), respectively, and with the CARELEC spectrograph (Lemaitre et al. 1990) attached to the 1.92 m telescope of the Observatoire de Haute Provence (OHP) (France).

Table 1 lists the characteristics of the instrumentation in the adopted set-up.

The observations at Loiano were performed using a 2.0 or 2.5 arcsec slit, depending on the seeing conditions, generally oriented E-W. Every galaxy spectrum was preceded and followed by an exposure of a HeAr lamp to secure the wavelength calibration. The exposure time ranged between 20 and 90 min (1999 run) according to the brightness of the target objects, or 15 min (2000 run) owed to the much higher quantum efficiency of the new EEV detector.

The observations at Cananea were carried out with a 1.9 arcsec slit, generally oriented N-S. Every galaxy spectrum was preceded and followed by an exposure of a XeNe lamp to secure the wavelength calibration. The exposure time ranged between 20 and 40 min according to the brightness of the target objects.

The observations at OHP were carried out with a 2.5 arcsec fixed slit, generally oriented E-W. Every galaxy spectrum was preceded and followed by an exposure of a HeAr lamp to secure the wavelength calibration. The exposure time ranged between 20 and 30 min according to the brightness of the target objects. In all runs the observations were obtained in nearly photometric conditions, with thin cirrus. The orientation of the slit was modified from the set-up given above when two adjacent objects were observable in the same exposure.

The data reduction was performed in the IRAF-PROS environment. After bias subtraction, when 3 or more frames of the same target were obtained, these were combined (after spatial alignment) using a median filter to help cosmic rays removal. Otherwise the cosmic rays were removed under visual inspection. The wavelength calibration was checked on known sky lines. These were found within ~ 1 Å from their nominal value, providing an estimate of the systematic uncertainty on the derived veloc-

ities of ~ 50 km s $^{-1}$. After subtraction of the sky background, one-dimensional spectra were extracted from the frames. These spectra were analyzed with either of two methods:

1) **individual line measurement:** all spectra taken at Loiano 2000 were inspected and emission/absorption lines were identified. Emission lines include H α , [NII] and [SII]. Absorption lines include the MgI, Ca-Fe and Na. The galaxy redshift was obtained from these individual measurements. If more than one line was identified, the galaxy redshift was derived as the weighted mean of the individual measurements, with weights proportional to the line intensities.

2) **cross correlation technique:** spectra obtained in all the remaining runs were analyzed using the cross-correlation technique of Tonry & Davis (1979). This method is based on a "comparison" between the spectrum of a galaxy whose redshift is to be determined, and a fiducial spectral template of a galaxy (or star) of appropriate spectral type to contain the wanted absorption/emission lines. The basic assumption behind this method is that the spectrum of a galaxy is well approximated by the spectrum of its stars, modified by the effects of the stellar motions inside the galaxy and by the systemic redshift. For this purpose high signal-to-noise spectra were taken of four template galaxies: M105 and M32 (absorption lines) and VCC1554 and IC342 (emission lines), which were converted to the restframe λ . The observed redshifts (V_{obs}) were not transformed to Heliocentric.

3. Results

The velocity measurements obtained in this work are listed in Table 2 (Virgo) and 3 (Coma) as follow:

Column 1: the CGCG (Zwicky et al. 1961-68) or VCC (Binggeli et al. 1985) designation.

Columns 2, 3: (B1950) celestial coordinates, measured with few arcsec uncertainty.

Column 4: morphological type as given in the VCC.

Column 5: photographic magnitude.

Column 6, 7: observed recessional velocity with uncertainty derived in this work. The latter quantity includes only statistical errors. The global uncertainty can be derived by adding in quadrature the systematic error of 50

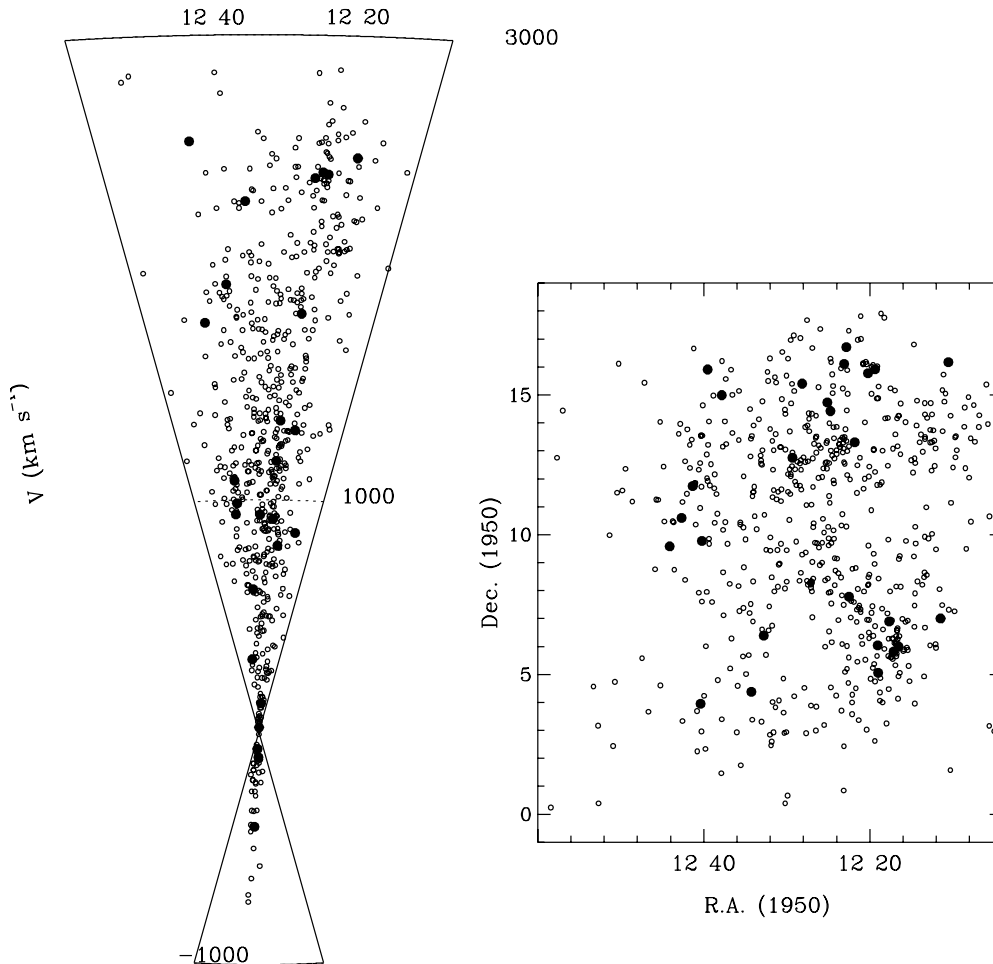


Fig. 1. The distribution in celestial coordinates of 639 Virgo galaxies with $V \leq 3000 \text{ km s}^{-1}$ (right) and a wedge diagram (left). The filled symbols represent measurements obtained in the present work.

km s^{-1} due to the uncertainty in the absolute wavelength calibration. Several absorption line spectra have statistical errors up to 900 km s^{-1} , reflecting a lack of strong features. These redshifts, however, are sufficient to derive a membership.

Column 8: type of lines (A=absorption; E=emission).

Column 9: observing run (L99=Loiano 1999, L00=Loiano 2000, Can=Cananea 2000, OHP=OHP 1999).

Column 10: old membership as given in the VCC (bk=background, m=member, -=possible member)(only for Table 2).

Column 10a: new membership.

Column 11, 12: previously available redshift, with reference.

Fig. 1 gives a representation in celestial coordinates of 639 galaxies in the VCC region with redshift $V \leq 3000 \text{ km s}^{-1}$ (panel a) and a wedge diagram (in the same velocity window) is given in panel b. Small symbols mark

galaxies taken from the literature, filled circles mark the measurements obtained in this work. Fig. 2 gives a representation in celestial coordinates of 913 galaxies in the VCC region with redshift $\leq 24000 \text{ km s}^{-1}$ (panel a) and a wedge diagram is given in panel b. Fig. 3 gives a representation in celestial coordinates of 1109 galaxies in the Coma region with measured redshift (top) and a wedge diagram is given (bottom). (Same use of symbols as in Figs. 1 and 2).

3.1. redshift completeness

The VCC catalogue contains 2096 galaxies brighter than $B_T = 20.0$. Of these only 913 have a redshift measurement so far. Even at brighter levels the redshift information is far from complete (see Tab. 4 for details). For example among the 849 galaxies with $B_T < 16.0$ there are still 69 with no spectra available. It is not surprising, though, that

Table 2. Parameters of the observed Virgo galaxies

Gal.	$RA(1950)$ <i>h m s</i>	$Dec(1950)$ <i>° ' "</i>	<i>Type</i>	B_T mag	V km s^{-1}	\pm	<i>Lines</i>	<i>Run</i>	<i>Memb</i>	<i>newMemb</i>	v_{att}	<i>ref</i>
(1)	(2)	(3)	(4)	(5)	(6)	(7)	(8)	(9)	(10)	(10a)	(11)	(12)
VCC0007	120645.60	114230.0	<i>Sc</i>	15.04	18675	425	<i>A</i>	<i>Can</i>	<i>bk</i>	<i>bk</i>		
VCC0014	120717.80	113205.0	<i>BCD?</i>	16.50	17891	35	<i>E</i>	<i>L00</i>	–	<i>bk</i>		
VCC0019	120740.80	132800.0	<i>BCD?</i>	16.50	6803	99	<i>E</i>	<i>L00</i>	–	<i>bk</i>		
VCC0045	120934.70	152315.0	<i>BCD?</i>	16.00	15236	36	<i>E</i>	<i>L00</i>	–	<i>bk</i>		
VCC0064	121008.50	114955.0	<i>Sab</i>	15.04	18142	336	<i>A</i>	<i>Can</i>	<i>bk</i>	<i>bk</i>		
VCC0074	121031.80	161024.0	<i>BCD?</i>	16.30	861	78	<i>E</i>	<i>Can</i>	–	<i>m</i>		
VCC0099	121128.90	70004.0	<i>Sa?</i>	14.81	2476	214	<i>E</i>	<i>L99</i>	–	<i>m</i>	2444	<i>GGH98</i>
VCC0196	121400.00	94624.0	<i>BCD?</i>	16.50	13024	57	<i>E</i>	<i>L00</i>	–	<i>bk</i>		
VCC0225	121439.00	83612.0	<i>BCD?</i>	17.00	21345	126	<i>E</i>	<i>L00</i>	–	<i>bk</i>		
VCC0249	121509.00	133930.0	<i>Sa</i>	14.61	7491	61	<i>E</i>	<i>Can</i>	<i>bk</i>	<i>bk</i>		
VCC0323	121633.20	60012.0	<i>Sa</i>	14.91	2402	358	<i>A</i>	<i>L99</i>	–	<i>m</i>	2756	<i>GGH98</i>
VCC0362	121709.00	54856.0	<i>Sa</i>	14.51	1300	304	<i>A</i>	<i>L99</i>	–	<i>m</i>	1536	<i>GGH98</i>
VCC0397	121739.00	65402.0	<i>dE?</i>	15.00	2411	809	<i>A</i>	<i>L99</i>	–	<i>m</i>	2495	<i>GGH98</i>
VCC0482	121900.80	50324.0	<i>S0a</i>	14.77	1802	709	<i>A</i>	<i>L99</i>	–	<i>m</i>	2170	<i>GGH98</i>
VCC0486	121903.80	60235.0	<i>S0a</i>	14.50	2386	252	<i>A</i>	<i>L99</i>	–	<i>m</i>	2498	<i>GGH98</i>
VCC0510	121922.80	155518.0	<i>dE</i>	15.13	804	151	<i>A</i>	<i>Can</i>	<i>m</i>	<i>m</i>		
VCC0541	121945.00	43348.0	<i>BCD</i>	16.00	23511	50	<i>E</i>	<i>L00</i>	–	<i>bk</i>		
VCC0573	122009.60	55454.0	<i>Sc</i>	15.20	23083	189	<i>E</i>	<i>Can</i>	<i>bk</i>	<i>bk</i>	23083	<i>NED</i>
VCC0583	122014.40	154636.0	<i>Im</i>	15.76	–72	475	<i>A</i>	<i>L99</i>	<i>m</i>	<i>m</i>		
VCC0723	122149.80	131824.0	<i>dS0?</i>	15.04	125	50	<i>A</i>	<i>L00</i>	–	<i>m</i>		
VCC0762	122230.00	74660.0	<i>dE</i>	15.30	1341	211	<i>A</i>	<i>Ohp</i>	<i>m</i>	<i>m</i>		
VCC0794	122250.40	164224.0	<i>dS0</i>	15.50	918	817	<i>A</i>	<i>Ohp</i>	<i>m</i>	<i>m</i>		
VCC0817	122306.00	160642.0	<i>dE</i>	15.00	1168	153	<i>A</i>	<i>Can</i>	<i>m</i>	<i>m</i>		
VCC0991	122445.90	142525.0	<i>dE</i>	14.70	–406	239	<i>A</i>	<i>L99</i>	<i>m</i>	<i>m</i>		
VCC1028	122506.60	144360.0	<i>dS0?</i>	15.70	21	158	<i>A</i>	<i>Ohp</i>	–	<i>m</i>		
VCC1174	122645.80	101246.0	<i>BCD?</i>	15.50	11840	52	<i>E</i>	<i>L99</i>	–	<i>bk</i>		
VCC1270	122743.80	84800.0	<i>Sa</i>	15.00	11687	440	<i>A</i>	<i>Can</i>	<i>bk</i>	<i>bk</i>		
VCC1304	122809.00	152412.0	<i>dS0</i>	15.50	–108	294	<i>A</i>	<i>L99</i>	<i>m</i>	<i>m</i>		
VCC1389	122919.80	124530.0	<i>dE</i>	15.91	936	193	<i>A</i>	<i>Can</i>	<i>m</i>	<i>m</i>		
VCC1395	122923.40	85248.0	<i>dE?</i>	16.20	22900	100	<i>E</i>	<i>L00</i>	–	<i>bk</i>		
VCC1423	122942.60	31630.0	<i>BCD?</i>	16.00	13079	98	<i>A</i>	<i>Can</i>	–	<i>bk</i>		
VCC1608	123247.60	62325.0	<i>E</i>	14.20	2285	193	<i>A</i>	<i>L99</i>	–	<i>m</i>	2464	<i>GGH98</i>
VCC1643	123321.00	60212.0	<i>S0</i>	15.20	12509	258	<i>A</i>	<i>Ohp</i>	–	<i>bk</i>	12563	<i>GGH98</i>
VCC1671	123359.60	62641.0	<i>dS0</i>	14.80	11608	809	<i>A</i>	<i>L99</i>	–	<i>bk</i>	11846	<i>GGH98</i>
VCC1687	123416.20	42242.0	<i>dE</i>	15.10	616	122	<i>A</i>	<i>Can</i>	–	<i>m</i>		
VCC1836	123749.80	145930.0	<i>dS0</i>	14.54	1927	148	<i>A</i>	<i>Can</i>	<i>m</i>	<i>m</i>		
VCC1849	123803.60	94942.0	<i>BCD?</i>	16.20	15905	50	<i>E</i>	<i>L00</i>	–	<i>bk</i>		
VCC1906	123932.20	155438.0	<i>S0</i>	15.70	314	138	<i>A</i>	<i>Can</i>	–	<i>m</i>		
VCC1927	124005.40	105024.0	<i>Sc</i>	14.91	20085	180	<i>A</i>	<i>Can</i>	<i>bk</i>	<i>bk</i>		
VCC1936	124014.40	94654.0	<i>dS0</i>	15.68	985	276	<i>A</i>	<i>Ohp</i>	<i>m</i>	<i>m</i>		
VCC1947	124023.30	35701.0	<i>dE</i>	14.56	1083	405	<i>A</i>	<i>L99</i>	–	<i>m</i>	944	<i>GGH98</i>
VCC1956	124036.00	35118.0	<i>S.</i>	15.10	14691	51	<i>E</i>	<i>L99</i>	–	<i>bk</i>	14659	<i>GGH98</i>
VCC1982	124119.20	114412.0	<i>dE</i>	15.30	938	464	<i>A</i>	<i>Ohp</i>	<i>m</i>	<i>m</i>		
VCC1997	124151.60	102742.0	<i>Sb</i>	15.10	9210	46	<i>E</i>	<i>Can</i>	<i>bk</i>	<i>bk</i>		
VCC2015	124240.20	103554.0	<i>BCD?</i>	16.20	2545	115	<i>E</i>	<i>L00</i>	–	<i>m</i>		
VCC2042	124407.20	93448.0	<i>dE</i>	14.84	1765	154	<i>A</i>	<i>Can</i>	<i>m</i>	<i>m</i>		
VCC2077	124604.50	110851.0	<i>Sab</i>	15.20	11860	225	<i>A</i>	<i>Can</i>	<i>bk</i>	<i>bk</i>		
VCC2082	124727.60	113206.0	<i>S.</i>	15.30	7421	26	<i>E</i>	<i>Can</i>	<i>bk</i>	<i>bk</i>		

Table 3. Parameters of the observed Coma galaxies

Gal.	<i>RA</i> (1950) <i>h m s</i>	<i>Dec</i> (1950) <i>° ' "</i>	<i>Type</i>	B_T mag	V km s ⁻¹	\pm	<i>Lines</i>	<i>Run</i>	<i>Memb</i>	v_{att}	<i>ref</i>
(1)	(2)	(3)	(4)	(5)	(6)	(7)	(8)	(9)	(10a)	(11)	(12)
127-028	113851.25	250457.3	S0	15.60	3518	330	A	L99	fg		
127-029N	113859.62	260956.6	E	16.30	7407	14	E	Can	m		
127-029S	113900.06	260926.5	E	16.30	6927	113	A	Can	m		
97-153W	114513.24	184955.0	S..	16.30	11156	20	E	Can	bk		
97-153E	114515.08	184936.7	S..	16.30	20261	112	E	Can	bk		
127-057S	114550.62	260223.9	S..	16.50	13666	75	E	Can	bk		
127-057N	114551.69	260251.3	S..	16.50	13718	15	E	Can	bk		
127-102	115130.07	232813.1	E	15.70	7799	139	A	Ohp	m		
128-028W	120405.12	260142.4	E	16.40	7353	198	A	Can	m		
128-028E	120406.94	260150.2	E	16.40	13788	143	A	Can	bk		
98-088	120903.25	201024.8	S0	15.70	6564	215	A	Ohp	m		
128-055	121122.87	220200.8	S0	15.70	7227	330	A	L99	m		
98-120	121341.37	194405.9	E	15.70	13208	202	A	Ohp	bk		
98-127	121409.85	183918.2	E	15.70	8954	203	A	Ohp	bk		
99-013	121638.07	193306.1	Sc	15.70	7297	16	E	Ohp	m		
128-083	121936.55	240846.0	E	15.70	10182	129	E	Ohp	bk		
128-083E	121939.64	240847.5	E	17.00	10292	164	A	Ohp	bk		
128-085	122150.98	212612.2	Sc	15.60	914	21	E	Ohp	fg		
99-066	122620.69	194525.9	Sb	15.70	13582	86	E	Ohp	bk		
129-003	122631.44	245429.9	Sc	15.70	14572	9	E	Ohp	bk		
99-067	122635.25	191652.4	E	15.70	14393	250	A	Ohp	bk		
159-087E	124810.87	274149.8	Sbc	15.70	12286	16	E	Ohp	bk		
160-036S	125435.00	305820.9	S0	16.00	15302	177	A	Can	bk		
160-036E	125438.62	305831.5	E	16.50	14880	185	A	Can	bk		
160-163S	131035.69	272401.1	E	16.50	17929	178	A	Can	bk		
160-163	131036.56	272421.7	S0a	15.70	18015	72	E	Can	bk		
161-029	131912.70	263359.0	Sb	15.70	4930	11	E	Ohp	m		
161-061S	132554.00	285542.1	S..	15.60	11281	32	E	Can	bk	11247	G99
161-061N	132554.69	285657.4	E	16.50	10564	165	A	Can	bk		

such relatively bright objects remain unmeasured because, given the vicinity of the Virgo cluster, galaxies in this magnitude range have low luminosities ($M_p > -15.0$). Given the known inverse proportionality between the luminosity and the surface brightness, they all correspond with extremely low surface brightness galaxies, which are much more difficult to observe spectroscopically than objects of similar magnitude which are further away. Furthermore, galaxies with missing spectra are almost entirely dEs, thus with featureless spectra. During the spectroscopical runs described in the present paper we have tried, unsuccessfully, to measure several of these objects: VCC 236 (dE), 452 (dE), 816 (dE), 1417 (dE), 1497 (dE), 1503 (dE), 1571 (dE), 1649 (dE), 1755 (dE), 1825 (dIm/dE), 1945 (dE), 1991 (dE), 2083 (dS0) with integration time ~ 30 min. We point out to those observers who wish to obtain successful spectra at 2m class telescopes to try with much longer exposures.

The redshift completeness is far better in the Coma-region, limited however to a brighter magnitude. Of the

1127 CGCG galaxies listed in the Coma region, 1082 have $B_T \leq 15.7$. Another 45 belong to multiple systems which were split in their individual components, each of them fainter than the catalogue limiting magnitude 15.7. Only 2/1082 galaxies with $B_T \leq 15.7$ and 18/1127 with $B_T \leq 16.5$ remain with unknown redshift, thus the sample is 98% complete.

An interesting example of a strong emission-line object in the background of the Coma supercluster is CGCG 127-057N which was observed at Cananea. The spectrum of this galaxy (see Fig.4) shows strong Balmer and [OIII] lines and weak [NII] and [SII]. The corresponding metallicity derived from $[OIII]/H\beta$, as prescribed by Edmunds & Pagel (1984) is: $12+\log(O/H)=8.16$.

3.2. membership

The membership to the Virgo cluster given in the VCC (members, possible-members, background) was estimated on purely morphological grounds (mostly on the surface

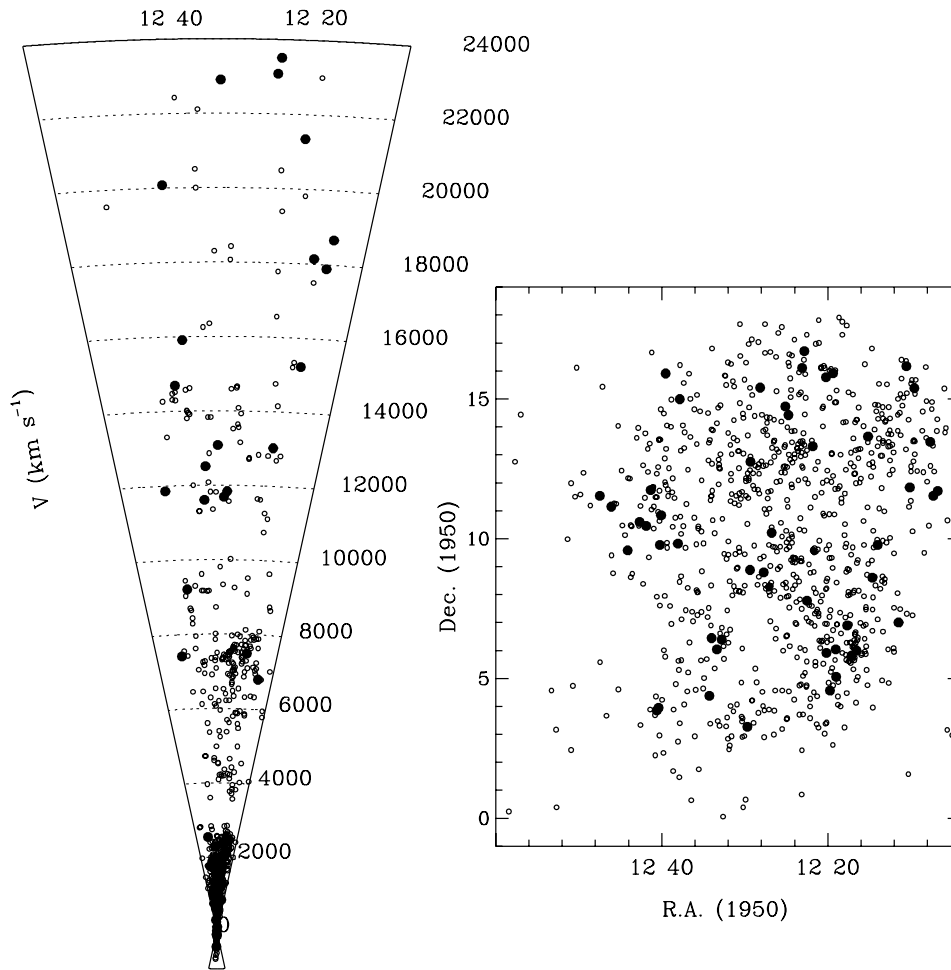


Fig. 2. The distribution in celestial coordinates of 913 Virgo galaxies with $V \leq 24000$ km s $^{-1}$ (right) and a wedge diagram (left) (same symbols as in Fig. 1).

Table 4. redshift completeness in the Virgo cluster

mag	tot	with z	%
≤ 15.0	549	546	99
≤ 16.0	849	780	92
≤ 17.0	1064	864	81
≤ 18.0	1323	903	68
≤ 19.0	1704	913	53
≤ 20.0	2096	916	43

brightness) by Binggeli et al. (1985). The new redshifts presented in this paper, in conjunction with two other recent sets of Virgo velocity measurements (Magri 1994) and GGH98), can be used to reassess this issue. We find that all objects listed in the VCC as "members" are confirmed

as such ($V < 3000$ km s $^{-1}$), stressing the high success-rate of the morphological estimate. "Possible members" are found with $V < 3000$ km s $^{-1}$ in 67 % of cases, the remaining being background objects. We have noticed that out of the 13 "Possible members" which are in fact high redshift objects, 10 were classified as possible BCDs (BCD?). These appear to be systematically emission-line blue giant objects, not dwarfs, nor compact galaxies (see Tab. 2).

As an example we give in Fig. 5 the rotation curve of one of them: VCC1849, which has a total rotational velocity up to 300 km s $^{-1}$, not typical of a dwarf galaxy. The rotation curve was derived at intermediate dispersion during the Loiano 2000 run with the slit oriented along the galaxy major axis. All objects classified as "Background" in the VCC are confirmed as such.

In summary, we obtained 76 new redshift measurements of galaxies, 48 of which are projected onto the Virgo cluster and 28 in the direction of the Coma-A1367 super-

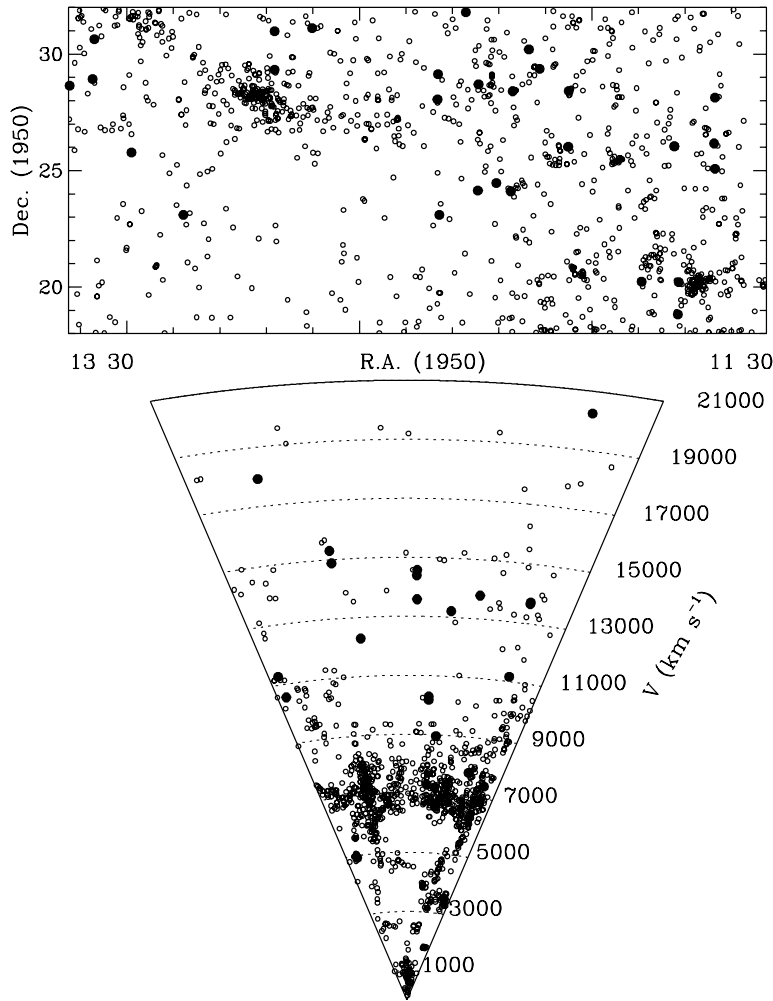


Fig. 3. The distribution in celestial coordinates of 1109 galaxies in the direction of the Coma supercluster with measured redshift (top) and a wedge diagram (bottom)(same symbols as in Fig. 1).

cluster. With these new data, the redshift completeness in the VCC region remains 92% for $B_T \leq 16.0$ and 68% for $B_T \leq 18.0$. All membership estimates, as given in the VCC, are confirmed. We remark that a large fraction of the possible members classified as BCDs?, are found to be giant emission-line galaxies well beyond the Virgo cluster.

The redshift completeness of CGCG galaxies in the direction of the Coma–A1367 supercluster is now 98%.

Acknowledgements. We wish to thank the TACS of the Loiano, Cananea and OHP telescopes for the generous amounts of time allocated to this project. G.G. wishes to thank his students for their contribution during the observations and the data reduction. This work could not be completed without the use of the NASA/IPAC Extragalactic Database (NED) which is operated by the Jet Propulsion Laboratory, Caltech under contract with NASA. L.C. has had support from CONACYT (México) research grant No. G-28586E.

References

- Binggeli B., Sandage A., & Tammann G., 1985, *AJ*, 90, 1681
- Binggeli B., Popescu C. & Tammann G., 1993, *AAS*, 98, 275
- Edmunds M., & Pagel B., 1984, *MNRAS*, 211, 507
- Haynes M., & Giovanelli R.: 1986, *ApJ*, 306, 466
- Hoffman L., Helou G., Salpeter E., Glosson J., & Sandage A., 1987, *ApJS*, 63, 247
- Hoffman G., Lewis B., Helou G., Salpeter E., Williams B. 1989, *ApJS*, 69, 65
- Hoffman G., Lewis B., & Salpeter E., 1995, *ApJ*, 441, 28
- Gavazzi G., Boselli A., Scodreggio M., Pierini D. & Belsole E., 1999a, *MNRAS*, 304, 595
- Gavazzi G., Carrasco L., & Galli R., 1999b, *AAS*, 136, 227 (G99)
- Grogin N., Geller M., & Huchra J., 1998, *ApJS*, 119, 277 (GGH98)
- Lemaitre G., Kohler D., Lacroix D., Meunier J., & Vin A., 1990, *A&A*, 228, 540
- Magri C., 1994, *ApJ*, 108, 896

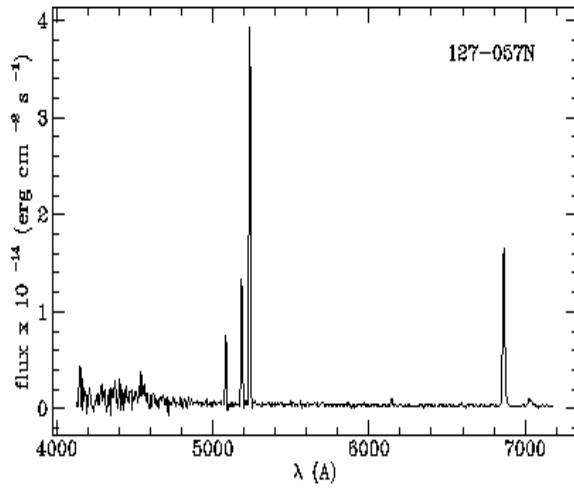


Fig. 4. The emission-line spectrum of 127-057N

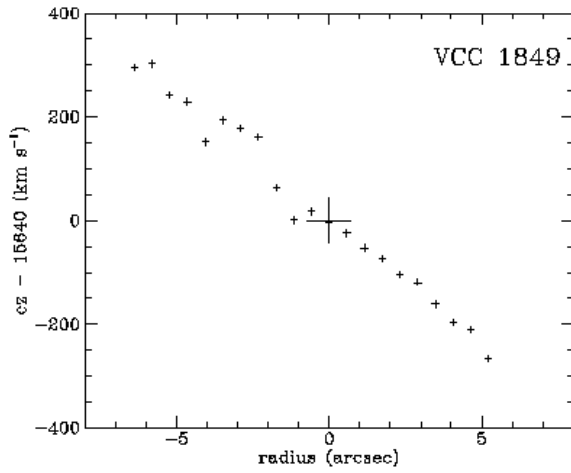


Fig. 5. The $H\alpha$ rotation curve of VCC1849

Sandage A., Binggeli B., & Tammann G., 1985, AJ, 90, 395
 Tonry J., and Davis M., 1979, AJ, 84, 1511
 Zwicky F., Herzog E., Karpowicz M., Koval C., & Wild P.,
 1961-1968, Catalogue of Galaxies and Clusters of Galaxies.
 (Pasadena: Caltech)(GCGC)